

# Cascaded Channel Estimation for Large Intelligent Metasurface Assisted Massive MIMO

Zhen-Qing He and Xiaojun Yuan, *Senior Member, IEEE*

**Abstract**—In this paper, we consider the problem of channel estimation for large intelligent metasurface (LIM) assisted massive multiple-input multiple-output (MIMO) systems. The main challenge of this problem is that the LIM with a large number of low-cost metamaterial antennas can only passively reflect the incident signal by a certain phase shift, and does not have any signal processing capability. We introduce a general framework for the estimation of the transmitter-LIM and LIM-receiver cascaded channel, and propose a three-stage algorithm that includes a sparse matrix factorization stage, a probabilistic ambiguity elimination stage, and a matrix completion stage. Simulation results illustrate that the proposed algorithm can achieve accurate channel estimation for LIM-assisted massive MIMO systems.

**Index Terms**—Bilinear factorization, channel estimation, large intelligent metasurface, massive MIMO, matrix completion.

## I. INTRODUCTION

MASSIVE multiple-input multiple-output (MIMO), as a promising technology for future wireless systems, has attracted growing research interest in both academia and industry over recent years. Although massive MIMO exhibits huge potentials to support a significantly large amount of mobile data traffic and wireless connections, implementing this system with large-scale antenna arrays in practice remains very challenging due to high hardware cost and increased power consumption. To achieve green and sustainable wireless networks, researchers have started looking into energy efficient techniques to improve the system performance, ranging from the utilization of energy efficient hardware components to the design of green resource allocation and transceiver signal processing algorithms.

Among the recent hardware technologies that promise significant reduction of energy consumption in wireless networks, the large intelligent metasurface (LIM) [1]–[3], a.k.a. the intelligent reflecting surface [4] or the reconfigurable intelligent surface [5], is a revolutionizing new technology that conceptually goes beyond contemporary massive MIMO communications. Recent years have witnessed the great success of metamaterial technologies in a wide range of applications including passive radar, imaging, and hologram, thanks to its great flexibility in manipulating electromagnetic waves. As an application of the metamaterial in wireless communications, the LIM with integrated electronics retains almost all the advantages of massive MIMO such as allowing for an unprecedented focusing of energy that enables highly efficient wireless charging and remote sensing. Note that traditional reflecting surfaces have a

variety of applications in radar and satellite communications, but their application in terrestrial wireless communication was not possible earlier. This is because these surfaces only had fixed phase shifters that could not adapt the induced phases with the time-varying channels that generally constitute the wireless propagation environments.

To achieve full potentials of LIM-assisted massive MIMO, the knowledge of channel state information (CSI) between the base station (BS) and the LIM and between the LIM and the user terminal, is required for reflect/passive beamforming [4], [6]. The main challenge of this problem is that the LIM, unlike the BS or the receiver, only passively reflects the electromagnetic waves, and does not have any signal processing capability. By leveraging the programmable property of the LIM and the low-rank structure of the massive MIMO channel, we formulate the BS-LIM and LIM-user cascaded channel estimation as a combined sparse matrix factorization and matrix completion problem. To solve the problem, we present a three stage algorithm which includes the matrix factorization stage, the ambiguity elimination stage, and the matrix completion stage. The proposed three stage algorithm includes the bilinear generalized approximate message passing (BiG-AMP) [7] for sparse matrix factorization, a probabilistic greedy pursuit for the ambiguity elimination, and a matrix completion algorithm using the Riemannian manifold gradient algorithm [8]. To the best of our knowledge, this is the first attempt to address the cascaded channel estimation problem for LIM-aided massive MIMO systems with all passive elements in the LIM. Note that the authors in [9] proposed a compressive sensing and training based deep learning method for the LIM-assisted MIMO channel estimation. Nevertheless, in [9] active antenna elements are implemented in the LIM to convert the challenging cascaded channel estimation problem into two conventional channel estimation problems.

**Notations:**  $\mathbb{E}\{\cdot\}$ ,  $\mathbb{V}\text{ar}\{\cdot\}$ ,  $\delta(\cdot)$ ,  $\mathbb{C}(\mathbb{R})$ ,  $(\cdot)^T$ ,  $(\cdot)^H$ ,  $(\cdot)^*$ , and  $\|\cdot\|_F$  denote the expectation operator, variance operator, Dirac delta function, space of complex (real) number, transpose, conjugate transpose, conjugate operation, and Frobenius norm, respectively (resp.). The  $(i, j)$ -th entry,  $i$ -th row, and  $j$ -th column of a matrix  $\mathbf{A}$ , are denoted by  $a_{i,j}$ ,  $\mathbf{a}_i^T$ , and  $\mathbf{a}_j$ , resp. We use  $\odot$  and  $\mathcal{CN}(\mu, \nu)$  to stand for the Hadamard product and the circularly-symmetric complex Gaussian distribution with mean  $\mu$  and variance  $\nu$ , resp.

## II. SYSTEM MODEL

Consider a LIM-assisted massive MIMO system, as shown in Fig. 1, where the LIM consists of  $N$  low-cost passive elements

Z.-Q. He and X. Yuan are with the Center for Intelligent Networking and Communications, the National Key Laboratory of Science and Technology on Communications, University of Electronic Science and Technology of China, Chengdu 611731, China (e-mail: zhenqinghe@uestc.edu.cn; xjyuan@uestc.edu.cn).

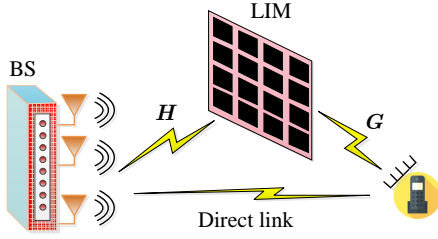


Fig. 1. A LIM assisted massive MIMO system.

and the BS is equipped with  $M$  transmit antennas to serve a number of user terminals, each equipped with  $L$  receive antennas. In particular, the LIM is deployed to assist the BS in communicating with the users. Without loss of generality, we consider the communication from the BS to a reference user. The baseband equivalent channels from the BS to the LIM and from the LIM to the user are resp. denoted by  $\mathbf{H} \in \mathbb{C}^{N \times M}$  and  $\mathbf{G} \in \mathbb{C}^{L \times N}$ . The direct-path channel component between the BS and the user is neglected due to unfavorable propagation conditions or can be estimated (and cancelled from the model) via conventional massive MIMO channel estimation methods (see e.g., [10]–[13]) by turning off the LIM. We assume a block-fading channel with coherence time  $T$ , i.e., the channel remains unchanged within each transmission block of length  $T$ . Then, the received signal of the reference user can be expressed as

$$\mathbf{y}[t] = \mathbf{G}(\mathbf{s}[t] \odot (\mathbf{H}\mathbf{x}[t])) + \mathbf{w}[t], t = 1, \dots, T \quad (1)$$

where  $\mathbf{x}[t]$  and  $\mathbf{w}[t]$  are resp. the transmitted signal and the additive noise drawn from  $\mathcal{CN}(\mathbf{0}, \sigma^2 \mathbf{I})$  at time  $t$ . The phase shift vector  $\mathbf{s}[t]$  of the LIM is defined as  $\mathbf{s}[t] \triangleq [s_{t,1}e^{j\theta_{t,1}}, \dots, s_{t,N}e^{j\theta_{t,N}}]^T$  where  $j \triangleq \sqrt{-1}$ , with  $\theta_{t,n} \in (0, 2\pi]$  and  $s_{t,n} \in \{0, 1\}$  representing the phase shift and the on/off state<sup>1</sup> of the  $n$ -th LIM reflect element at time  $t$ , resp. By summarizing all the  $T$  samples in a transmission block, the received signal can be recast as

$$\mathbf{Y} = \mathbf{G}(\mathbf{S} \odot (\mathbf{H}\mathbf{X})) + \mathbf{W} \quad (2)$$

where  $\mathbf{Y} \triangleq [\mathbf{y}[1], \dots, \mathbf{y}[T]] \in \mathbb{C}^{L \times T}$ ,  $\mathbf{W} \triangleq [\mathbf{w}[1], \dots, \mathbf{w}[T]] \in \mathbb{C}^{L \times T}$ ,  $\mathbf{S} \triangleq [\mathbf{s}[1], \dots, \mathbf{s}[T]] \in \mathbb{C}^{N \times T}$ , and  $\mathbf{X} \triangleq [\mathbf{x}[1], \dots, \mathbf{x}[T]] \in \mathbb{C}^{M \times T}$ . A smart programmable controller is built in the LIM to adaptively adjust the states and the phases of the LIM based on environmental changes, usually referred to as passive beamforming or reflect beamforming [4].

The BS-LIM channel matrix  $\mathbf{H}$  is assumed to have a low-rank structure, i.e.,  $\text{rank}(\mathbf{H}) = R \ll \min\{N, M\}$ . Similar low-rank properties have been previously exploited in modeling massive MIMO channels under far-field and limited-scattering assumptions [15], [16]. Meanwhile, we assume that the channel matrix  $\mathbf{G}$  between the LIM and the user is full rank. This full-rank property can be justified, e.g., by the rich-scattering assumption of the LIM-user communication environment [17], or by the near-field line-of-sight channel modelling [18]. Of course, there are practical scenarios where  $\mathbf{G}$  is also a low-rank

<sup>1</sup>The state “off” of a LIM reflect element means that there is only structure-mode reflection generated as if the element is a conducting object, whereas the state “on” means that there are both structure-mode reflection and antenna-mode reflection [14]. Note that the structure-mode can be absorbed into the direct link in channel modelling.

matrix. In this case, the low-rank property of  $\mathbf{G}$  can be further exploited to improve the performance of channel estimation. However, this is out of the scope of the paper.

### III. PROBLEM FORMULATION

The CSI of the BS-LIM and LIM-user links is required in reflect beamforming [4], as well as in passive beamforming and information transfer [6]. In general, in [4], [6] the phase shift vectors  $\{\mathbf{s}[t]\}$  are set as a constant vector in each transmission block<sup>2</sup>, i.e.,

$$\mathbf{s}[t] = \mathbf{s}, t = 1, \dots, T.$$

Then, the signal model in (2) reduces to

$$\mathbf{Y} = \mathbf{G}\text{diag}\{\mathbf{s}\}\mathbf{H}\mathbf{X} + \mathbf{W}. \quad (3)$$

Clearly, we have

$$\mathbf{G}\text{diag}\{\mathbf{s}\}\mathbf{H} = \mathbf{G}'\text{diag}\{\mathbf{s}\}\mathbf{H}' \quad (4)$$

where  $\mathbf{G}' \triangleq \mathbf{G}\Phi$  and  $\mathbf{H}' \triangleq \Phi^{-1}\mathbf{H}$  are effective channels, and  $\Phi$  is a diagonal matrix with non-zero diagonal entries. This implies that the optimization of  $\mathbf{s}$  based on  $\mathbf{G}$  and  $\mathbf{H}$  yields the same result as that based on  $\mathbf{G}'$  and  $\mathbf{H}'$ . Thus, the optimization of  $\mathbf{s}$  for reflect beamforming in (3) requires the knowledge of  $\mathbf{G}$  and  $\mathbf{H}$  up to the ambiguity of a diagonal matrix  $\Phi$ . In other words, we need to estimate the cascaded channel  $\mathbf{G}$  and  $\mathbf{H}$  up to the ambiguity in (4) by an appropriate design of the training signals  $\{\mathbf{s}[t]\}$  and  $\{\mathbf{x}[t]\}$ .

### IV. PROPOSED CASCADED CHANNEL ESTIMATION ALGORITHM

We now address the cascaded channel estimation problem formulated in the preceding section. Note that setting  $\mathbf{s}[t]$  as a constant in a transmission block as in (3) does not work for the cascaded channel estimation. In that case, for given  $\mathbf{S}$  and  $\mathbf{X}$ , the estimation of  $\mathbf{G}$  and  $\mathbf{H}$  from  $\mathbf{Y}$  in (3) can be interpreted as an affine matrix factorization problem [19]. The condition that  $\mathbf{H}$  is a low-rank matrix is not enough to ensure the successful recovery of  $\mathbf{G}$  and  $\mathbf{H}$  from  $\mathbf{Y}$  even if the ambiguity in (4) is allowed. As such, we propose to employ a varying  $\mathbf{s}[t]$  in the design of training signals, as detailed below.

The system model in (2) can be rewritten as

$$\mathbf{Y} = \mathbf{G}\mathbf{Z} + \mathbf{W} \quad (5)$$

where  $\mathbf{Z} = \mathbf{S} \odot (\mathbf{H}\mathbf{X})$ . To facilitate the channel estimation, we describe the construction of pilot signals  $\mathbf{S}$  and  $\mathbf{X}$  as follows. For the LIM pilots, we generate  $\{s_{t,n}\}$  independently from a bernoulli distribution  $\text{Bernoulli}(\lambda)$  with  $\lambda$  being the probability of taking the value of 1, and generate  $\{\theta_{t,n}\}$  from the standard uniform distribution within  $(0, 2\pi]$ . For the BS pilots, we require that  $\mathbf{X}$  is a full-rank matrix, i.e.,  $\text{rank}(\mathbf{X}) = \max(M, T)$ .

From the construction of  $\mathbf{S}$ , we see that  $\mathbf{Z}$  in (5) is a sparse matrix. Thus, we can recover  $\mathbf{G}$  and  $\mathbf{Z}$  from  $\mathbf{Y}$  via bilinear sparse matrix factorization techniques, such as BiG-AMP [7].

<sup>2</sup>In reflect beamforming, there is no need to change the value of  $\mathbf{s}[t]$  unless the channel changes.

Note that the sparse matrix factorization suffers from the phase and permutation ambiguities [13], [19]. That is, if  $(\hat{\mathbf{G}}, \hat{\mathbf{Z}})$  is a solution to the factorization problem, then  $(\hat{\mathbf{G}}\Phi\Pi, \Pi^T\Phi^{-1}\hat{\mathbf{Z}})$  is also a valid solution, where  $\Phi$  is a diagonal matrix, and  $\Pi$  is an arbitrary permutation matrix. Recall that there is no need to eliminate the phase ambiguity  $\Phi$  based on (5) and the discussions therein. Thus, the next step of the channel estimation algorithm is to eliminate the permutation ambiguity  $\Pi$  based on the knowledge of the LIM pilot matrix  $\mathbf{S}$  (since each row  $n$  of  $\mathbf{S}$  gives a unique identity to the  $n$ -th reflect element of the LIM). Denote by  $\hat{\Pi}$  an estimate of  $\Pi$ . Then, the estimates of  $\mathbf{G}$  and  $\mathbf{Z}$  after removing the permutation ambiguity are resp. given by  $\hat{\mathbf{G}}\hat{\Pi}$  and  $\hat{\Pi}^T\hat{\mathbf{Z}}$ . Based on that, the last step of the channel estimation algorithm is to retrieve  $\mathbf{H}$  from  $\hat{\Pi}^T\hat{\mathbf{Z}}$  together with the fact that  $\mathbf{H}$  is a low-rank matrix. The overall channel estimation algorithm is referred to as the joint bilinear factorization and matrix completion (JBF-MC) algorithm presented in Algorithm 1. The details of the JBF-MC algorithm are explained in the following subsections.

#### A. Sparse Matrix Factorization

For the bilinear matrix factorization problem (5), we adopt the BiG-AMP algorithm [7] to approximately solve the following maximum *a posteriori* (MAP) estimation problem:

$$\begin{aligned} (\hat{\mathbf{G}}, \hat{\mathbf{Z}}) &= \arg \max_{\mathbf{G}, \mathbf{Z}} p(\mathbf{G}, \mathbf{Z} | \mathbf{Y}) \\ &= \arg \max_{\mathbf{G}, \mathbf{Z}} p(\mathbf{Y} | \mathbf{B}) p(\mathbf{G}) p(\mathbf{Z}) \end{aligned} \quad (6)$$

where  $\mathbf{B} \triangleq \mathbf{G}\mathbf{Z}$ , and the likelihood  $p(\mathbf{Y} | \mathbf{B})$  is separable and given as

$$p(\mathbf{Y} | \mathbf{B}) = \prod_{l=1}^L \prod_{t=1}^T p(y_{l,t} | b_{l,t}) \quad (7)$$

$$= \prod_{l=1}^L \prod_{t=1}^T \exp(-|y_{l,t} - b_{l,t}|^2 / \sigma). \quad (8)$$

We choose independent Gaussian priors for  $\mathbf{G}$  and independent Bernoulli-Gaussian priors for  $\mathbf{Z}$ , i.e.,

$$p(\mathbf{G}) = \prod_{l=1}^L \prod_{n=1}^N \mathcal{CN}(g_{l,n}; 0, \nu_g) \quad (9)$$

$$p(\mathbf{Z}) = \prod_{n=1}^N \prod_{t=1}^T (1 - \lambda) \delta(z_{n,t}) + \lambda \mathcal{CN}(z_{n,t}; 0, \nu_z) \quad (10)$$

where  $\nu_g$  and  $\nu_z$  are resp. the average power of the channel matrix  $\mathbf{G}$  and non-zero coefficients of  $\mathbf{Z}$ ;  $\lambda$  is the sparsity level (sampling rate) of  $\mathbf{Z}$ .

The BiG-AMP algorithm is a computationally efficient iterative procedure by leveraging the approximate message passing to solve the MAP inference problem (6). Details of the BiG-AMP can be found in Lines 1 to 22 of Algorithm 1. Specifically, in each iteration, the means and variances of  $\{g_{l,n}\}$  and  $\{z_{n,t}\}$  in Lines 16 to 19 are resp. calculated with respect to the approximate marginal posterior distributions:

$$\hat{p}^{(i)}(g_{l,n}) \propto p(g_{l,n}) e^{-|g_{l,n} - \hat{g}_{l,n}(i)|^2 / v_{l,n}^g(i)} \quad (11)$$

$$\hat{p}^{(i)}(z_{n,t}) \propto p(z_{n,t}) e^{-|z_{n,t} - \hat{z}_{n,t}(i)|^2 / v_{n,t}^z(i)}. \quad (12)$$

---

#### Algorithm 1: JBF-MC algorithm

---

**Input:**  $\mathbf{Y}, \mathbf{S}, \mathbf{X}$ , prior distributions  $p(\mathbf{G})$  and  $p(\mathbf{Z})$

% sparse matrix factorization via BiG-AMP

```

1: Initialization:  $\forall l, n, t$ : generate  $g_{l,n}$  from  $p(g_{l,n})$ ,  $v_{l,n}^g(1) = \nu_g$ ,
    $\hat{z}_{n,t}(1) = \mathbb{E}(z_{n,t})$ ,  $v_{n,t}^z(1) = \lambda \nu_z$ , and  $\hat{u}_{l,t}(1) = 0$ 
2: for  $i = 1, \dots, I_{\max}$  % outer iteration
3:   for  $j = 1, \dots, J_{\max}$  % inner iteration
4:      $\forall l, t$ :  $\bar{v}_{l,t}^p(i) = \sum_{n=1}^N |\hat{g}_{l,n}(i)|^2 v_{n,t}^z(i) + v_{l,n}^g(i) |\hat{z}_{n,t}(i)|^2$ 
5:      $\forall l, t$ :  $\bar{p}_{l,t}(i) = \sum_{n=1}^N \hat{g}_{l,n}(i) \hat{z}_{n,t}(i)$ 
6:      $\forall l, t$ :  $v_{l,t}^p(i) = \bar{v}_{l,t}^p(i) + \sum_{n=1}^N v_{l,n}^g(i) v_{n,t}^z(i)$ 
7:      $\forall l, t$ :  $\hat{p}_{l,t}(i) = \bar{p}_{l,t}(i) - \hat{u}_{l,t}(i-1) \bar{v}_{l,t}^p(i)$ 
8:      $\forall l, t$ :  $v_{l,t}^b(i) = \sigma v_{l,t}^p(i) / [v_{l,t}^p(i) + \sigma]$ 
9:      $\forall l, t$ :  $\hat{b}_{l,t}(i) = v_{l,t}^p(i) [y_{l,t} - \hat{p}_{l,t}(i)] / [v_{l,t}^p(i) + \sigma^2] + \hat{p}_{l,t}(i)$ 
10:     $\forall l, t$ :  $v_{l,t}^u(i) = [1 - v_{l,t}^z(i) / v_{l,t}^p(i)] / v_{l,t}^p(i)$ 
11:     $\forall l, t$ :  $\hat{u}_{l,t}(i) = [\hat{b}_{l,t}(i) - \hat{p}_{l,t}(i)] / v_{l,t}^u(i)$ 
12:     $\forall l, n$ :  $v_{l,n}^g(i) = [\sum_{t=1}^T |\hat{z}_{n,t}(i)|^2 v_{l,t}^u(i)]^{-1}$ 
13:     $\forall l, n$ :  $\hat{g}_{l,n}(i) = \hat{g}_{l,n}(i) [1 - v_{l,n}^g(i) \sum_{t=1}^T v_{n,t}^z(i) v_{l,t}^u(i)]$ 
   +  $v_{l,n}^g(i) \sum_{t=1}^T \hat{z}_{n,t}(i) \hat{s}_{l,t}(i)$ 
14:     $\forall n, t$ :  $v_{n,t}^r(i) = [\sum_{l=1}^L |\hat{g}_{l,n}(i)|^2 v_{l,t}^u(i)]^{-1}$ 
15:     $\forall n, t$ :  $\hat{r}_{n,t}(i) = \hat{z}_{n,t}(i) (1 - v_{n,t}^r(i) \sum_{l=1}^L v_{l,n}^g(i) v_{l,t}^u(i))$ 
   +  $v_{n,t}^r(i) \sum_{l=1}^L \hat{g}_{l,n}(i) \hat{u}_{l,t}(i)$ 
16:     $\forall l, n$ :  $\hat{g}_{l,n}(i+1) = \mathbb{E}\{g_{l,n} | \hat{g}_{l,n}(i), v_{l,n}^g(i)\}$ 
17:     $\forall l, n$ :  $v_{l,n}^g(i+1) = \mathbb{V}\text{ar}\{g_{l,n} | \hat{g}_{l,n}(i), v_{l,n}^g(i)\}$ 
18:     $\forall n, t$ :  $\hat{z}_{n,t}(i+1) = \mathbb{E}\{z_{n,t} | \hat{r}_{n,t}(i), v_{n,t}^r(i)\}$ 
19:     $\forall n, t$ :  $v_{n,t}^z(i+1) = \mathbb{V}\text{ar}\{z_{n,t} | \hat{r}_{n,t}(i), v_{n,t}^r(i)\}$ 
   if a certain stopping criterion is met, stop
20:   end for
21:    $\forall l, n, t$ :  $\hat{g}_{l,n}(i) = \hat{g}_{l,n}(i+1)$ ,  $\nu_{l,n}^g(i) = \nu_{l,n}^g(i+1)$ ,
    $\hat{z}_{n,t}(i) = \hat{z}_{n,t}(i+1)$ ,  $\nu_{n,t}^z(i) = \nu_{n,t}^z(i+1)$ 
22: end for
% permutation ambiguity elimination via greedy pursuit
23: Initialization:  $\Pi = \mathbf{0}$ ,  $\Gamma_0 = \emptyset$ 
24: for  $n = 1, \dots, N$  do
25:    $\forall n' \in \mathcal{N}$ , calculate  $P(\check{\mathbf{s}}_n = \mathbf{s}_{n'})$  via (17)-(20)
26:    $\hat{n} = \arg \max_{n' \in \mathcal{N} / \Gamma_{n-1}} P(\check{\mathbf{s}}_n = \mathbf{s}_{n'})$ 
27:    $\Pi(n, n') = 1$ ;  $\Gamma_n = \Gamma_{n-1} \cup \{\hat{n}\}$ 
28: end for
29:  $\tilde{\mathbf{G}} = \hat{\mathbf{G}}\Pi^T$  and  $\tilde{\mathbf{Z}} = \Pi\hat{\mathbf{Z}}$ 
% matrix completion via RGrad
30: Initialization:  $k = 0$  and  $\mathbf{A}(0) = \mathbf{0}$ 
31: repeat
32:    $\mathbf{Q}(k) = \mathbf{S} \odot (\tilde{\mathbf{Z}} - \mathbf{A}(k))$ 
33:    $\alpha(k) = \frac{\|\mathcal{P}_{\mathbf{S}(k)}(\mathbf{Q}(k))\|_F^2}{\|\mathbf{S} \odot (\mathcal{P}_{\mathbf{S}(k)}(\mathbf{Q}(k)))\|_F^2}$ 
34:    $\mathbf{W}(k) = \mathbf{A}(k) + \alpha(k) \mathcal{P}_{\mathbf{S}(k)}(\mathbf{Q}(k))$ 
35:    $\mathbf{A}(k+1) = \mathcal{H}_r(\mathbf{W}(k))$ 
36:    $k \leftarrow k + 1$ 
37: until a certain stopping criterion is met
38:  $\tilde{\mathbf{H}} = \tilde{\mathbf{A}}\mathbf{X}^\dagger$  with  $\tilde{\mathbf{A}} = \mathbf{A}(k+1)$ 
Output:  $\tilde{\mathbf{G}}$  and  $\tilde{\mathbf{H}}$ 

```

---

It is worth noting that the K-SVD (K-means singular value decomposition) [20] and the SPAMS (SPArse Modeling Software) [21] can be used to solve the bilinear factorization problem (5). However, these algorithms perform much worse than the BiG-AMP algorithm, as seen from the numerical results presented in Section V.

### B. Permutation Ambiguity Elimination

Note that a permutation matrix is a square binary matrix that has exactly one entry of 1 in each row and in each column, and 0s elsewhere. That is, the pattern (the positions of zero and non-zero entries) of BiG-AMP output  $\tilde{\mathbf{Z}}$  should match the pattern of the given  $\mathbf{S}$ . Let  $\Phi$  and  $\Pi$  resp. be the phase and permutation ambiguities contained in the BiG-AMP outputs  $\hat{\mathbf{G}}$  and  $\hat{\mathbf{Z}}$ . That is,  $\hat{\mathbf{G}}$  and  $\hat{\mathbf{Z}}$  are resp. the estimates of  $\check{\mathbf{G}} \triangleq \mathbf{G}\Pi^T\Phi^{-1}$  and  $\check{\mathbf{Z}} \triangleq \Phi\Pi\mathbf{Z}$ . Define by  $\check{\mathbf{S}}$  the state of  $\check{\mathbf{Z}}$  with

$$\check{s}_{n,t} \triangleq \begin{cases} 1, & \check{z}_{n,t} \neq 0 \\ 0, & \check{z}_{n,t} = 0. \end{cases} \quad (13)$$

With  $\check{\mathbf{Z}} \triangleq \Phi\Pi\mathbf{Z}$ , the relationship between  $\check{\mathbf{S}}$  and  $\mathbf{S}$  is

$$\check{\mathbf{S}} = \Pi\mathbf{S} \quad (14)$$

or equivalently

$$\check{s}_n^T = \pi_n^T \mathbf{S} = \mathbf{s}_{n'}^T, n \in \mathcal{N} \quad (15)$$

where  $\mathcal{N} \triangleq \{1, \dots, N\}$ ,  $\check{s}_n^T$  is the  $n$ -th row of  $\check{\mathbf{S}}$ , and  $n'$  satisfies that the  $(n, n')$ -th element of  $\Pi$ , i.e.,  $\pi_{n,n'} = 1$ . From Algorithm 1, the output distribution of each  $\check{z}_{n,t}$  of the BiG-AMP is given as

$$\begin{aligned} \hat{p}(\check{z}_{n,t}) &\propto p(\check{z}_{n,t}) e^{-|\check{z}_{n,t} - \hat{r}_{n,t}|^2 / v_{n,t}^r} \\ &= c_{n,t} \mathcal{CN}\left(\check{z}_{n,t}; \frac{\hat{r}_{n,t} \nu_z}{v_{n,t}^r + \nu_z}, \frac{v_{n,t}^r \nu_z}{v_{n,t}^r + \nu_z}\right) + (1 - c_{n,t}) \delta(\check{z}_{n,t}) \end{aligned}$$

where

$$c_{n,t} = \left(1 + \frac{(1 - \lambda) \mathcal{CN}(0; \hat{r}_{n,t}, v_{n,t}^r)}{\lambda \mathcal{CN}(0; \hat{r}_{n,t}, v_{n,t}^r + \nu_z)}\right)^{-1}. \quad (16)$$

Therefore, we have

$$P(\check{s}_{n,t} = 0 | \check{z}_{n,t} \sim \hat{p}(\check{z}_{n,t})) = c_{n,t} \quad (17)$$

$$P(\check{s}_{n,t} = 1 | \check{z}_{n,t} \sim \hat{p}(\check{z}_{n,t})) = 1 - c_{n,t}. \quad (18)$$

The probability of  $\check{s}_n = \mathbf{s}_{n'}$  is then given by

$$P(\check{s}_n = \mathbf{s}_{n'}) = \prod_{t=1}^T P(\check{s}_{n,t} = \mathbf{s}_{n',t} | \check{z}_{n,t} \sim \hat{p}(\check{z}_{n,t})) \quad (19)$$

Thus, we can find each row of the permutation matrix  $\Pi$  via

$$\hat{\pi}_n = \mathbf{e}_{\hat{n}} \text{ with } \hat{n} = \arg \max_{n'} P(\check{s}_n = \mathbf{s}_{n'}) \quad (20)$$

where  $\mathbf{e}_{\hat{n}} \in \mathbb{R}^N$  is the standard basis vector with its only non-zero entry (that is equal to 1) at the  $\hat{n}$ -th position. Note that directly using (20) may result in identical rows of  $\hat{\Pi}$ , leading to a rank-deficient matrix. To avoid this issue, we use a greedy pursuit strategy by removing the previous selections, as outlined in Lines 23 to 28 of Algorithm 1.

With the permutation matrix  $\hat{\Pi}$ , we obtain the estimates of  $\mathbf{G}$  and  $\mathbf{Z}$  after permutation ambiguity elimination as

$$\tilde{\mathbf{G}} = \hat{\mathbf{G}} \hat{\Pi}^T \text{ and } \tilde{\mathbf{Z}} = \hat{\Pi} \hat{\mathbf{Z}}. \quad (21)$$

### C. Matrix Completion

We now recover the missing entries of  $\tilde{\mathbf{Z}}$  by using the low-rank property of the original  $\mathbf{Z}$ . We employ the Riemannian gradient (RGrad) algorithm [8] to solve the matrix completion problem, which is summarized in Lines 30 to 37 of Algorithm 1. The RGrad algorithm is to solve the following low-rank completion problem:

$$\min_{\mathbf{A}} \frac{1}{2} \|\mathbf{S} \odot (\mathbf{A} - \tilde{\mathbf{Z}})\|_F^2 \text{ subject to } \text{rank}(\mathbf{A}) = r. \quad (22)$$

In Lines 33 and 34 of JBF-MC,  $\mathcal{P}_{\mathcal{S}(k)}$  denotes the projection to the left singular vector subspace, denoted by  $\mathcal{S}(k)$ , of the current estimate  $\mathbf{A}(k)$ . In Line 35,  $\mathcal{H}_r(\mathbf{W})$  is the hard-thresholding operator for the best rank- $r$  approximation of the associated SVD, i.e.,

$$\mathcal{H}_r(\mathbf{W}) \triangleq \mathbf{U} \Sigma_r \mathbf{V}^H, \Sigma_r(i, i) = \begin{cases} \Sigma(i, i), & i \leq r \\ 0, & i > r \end{cases} \quad (23)$$

where  $\mathbf{W} \triangleq \mathbf{U} \Sigma \mathbf{V}^H$  is the SVD of  $\mathbf{W}$ . Finally, the estimate of the channel matrix  $\mathbf{H}$  can be computed as

$$\hat{\mathbf{H}} = \hat{\mathbf{A}} \mathbf{X}^\dagger \quad (24)$$

where  $\mathbf{X}^\dagger = (\mathbf{X} \mathbf{X}^H)^{-1} \mathbf{X}$  is the Moore-Penrose inverse and  $\hat{\mathbf{A}}$  is output of the RGrad algorithm.

## V. SIMULATION RESULTS

We carry out experiments to test the performance of the proposed JBF-MC algorithm for the cascaded channel estimation of LIM-aided massive MIMO systems. The test signal model is generated according to (1). By the Rayleigh fading assumption, the LIM-user channel matrix  $\mathbf{G}$  is generated from  $\mathcal{CN}(0, 1)$ . The array structures at the BS and the LIM are assumed to be a half-wavelength uniform linear array (ULA). Following [12], [13], [18], the BS-LIM channel matrix  $\mathbf{H}$  is generated by

$$\mathbf{H} = \sum_{r=1}^R \alpha_r \mathbf{a}_L(\psi_r) \mathbf{a}_B^H(\vartheta_r) \quad (25)$$

where  $\mathbf{a}_L(\psi_p) \in \mathbb{C}^N$  and  $\mathbf{a}_B(\vartheta_p) \in \mathbb{C}^M$  are the steering vectors of the ULA at the LIM and the BS, resp. In each trial, the angular parameters  $\psi_r$  and  $\vartheta_r$  follow from the uniform distribution within  $(0, 1]$ , and the path coefficients  $\{\alpha_r\}$  are independently drawn from  $\mathcal{CN}(0, 1)$ . We assume that the number of paths, i.e.,  $R$ , is small such that the channel matrix  $\mathbf{H}$  has a low-rank structure to assist the cascaded channel estimation. The pilot symbols in  $\mathbf{X}$  are generated from  $\mathcal{CN}(0, 1)$  and the signal-to-noise ratio (SNR) is defined as  $10 \log_{10}(1/\sigma)$  dB. The estimation performance is evaluated in terms of the normalized mean-square-error (NMSE). All the results are obtained by averaging 500 independent trials except for the phase transition tests. Note that the outputs  $\tilde{\mathbf{G}}$  and  $\tilde{\mathbf{H}}$  of the proposed algorithm still contain phase ambiguities. The phase ambiguities are eliminated based on the true values of  $\mathbf{G}$  and  $\mathbf{H}$  in the calculation of the NMSEs. In the sparse matrix factorization stage, to benchmark our algorithm for the estimation of  $\mathbf{G}$ , we adopt the K-SVD [20] and the SPAMS [21] for comparison. In all simulations, we set  $L = 70$  and  $M = N = 64$ . For matrix

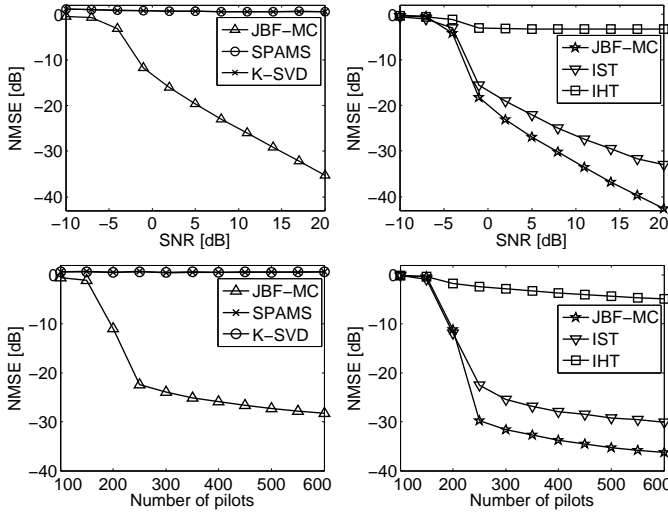


Fig. 2. NMSEs of  $\mathbf{G}$  (left subplots) and  $\mathbf{H}$  (right subplots) versus the SNR and the number of pilots with  $L = 70$  and  $M = N = 64$ .

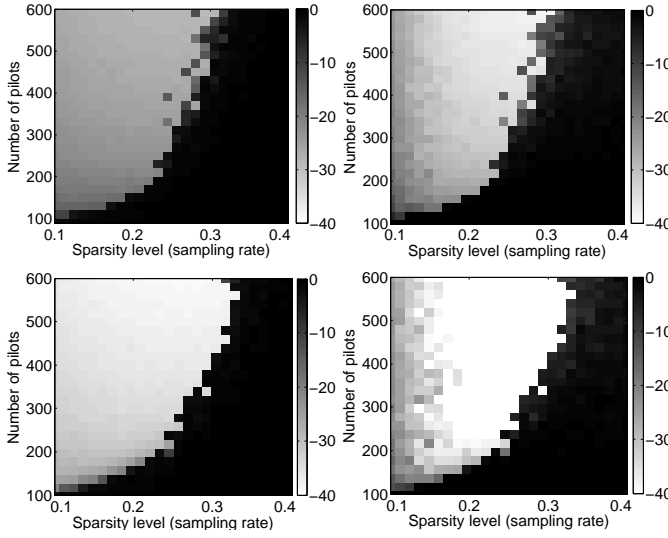


Fig. 3. Phase transitions (in NMSE) of  $\mathbf{G}$  (left subplots) and  $\mathbf{H}$  (right subplots) versus the sparsity level and the number of pilots. The upper subplots are for SNR = 10 dB and the lower subplots for SNR = 20 dB.

completion, we also use the IHT (iterative hard thresholding) and the IST (iterative soft thresholding) [22] to estimate  $\mathbf{H}$ .

The NMSEs versus the SNR and the number of pilots are depicted in Fig. 2. It is seen that the proposed approach exhibits a significant performance gain over the baseline methods, especially for the estimation of  $\mathbf{G}$ . Fig. 3 shows the phase transition of the channel estimation NMSEs versus the sparsity level and the number of pilots by averaging 50 trials. We observe from figs. 2 and 3 that the estimation of  $\mathbf{H}$  has a lower NMSE than that of  $\mathbf{G}$ . This is because  $\mathbf{Z}$  has a sparse structure (only a few non-zero entries) to be exploited in estimating  $\mathbf{H}$ .

## VI. CONCLUSIONS

In this work, we considered the cascaded channel estimation for the LIM-assisted massive MIMO systems. We introduced a general framework for this problem by leveraging a combined bilinear factorization and matrix completion, and presented a three-stage algorithm that includes a generalized bilinear message passing stage, an ambiguity elimination stage, and a matrix

completion stage. We provided experimental evidences that the proposed approach achieves an accurate channel estimation for the LIM-aided massive MIMO systems.

## REFERENCES

- [1] C. Liaskos, S. Nie, A. Tsioliaridou, A. Pitsillides, S. Ioannidis, and I. Akyildiz, "A new wireless communication paradigm through software-controlled metasurfaces," *IEEE Commun. Mag.*, vol. 56, no. 9, pp. 162–169, Sep. 2018.
- [2] S. Hu, F. Rusek, and O. Edfors, "Beyond massive MIMO: The potential of data transmission with large intelligent surfaces," *IEEE Trans. Signal Process.*, vol. 66, no. 10, pp. 2746–2758, May 2018.
- [3] M. Di Renzo, M. Debbah, D.-T. Phan-Huy *et al.* (Mar. 2019) Smart radio environments empowered by AI reconfigurable metasurfaces: An idea whose time has come. [Online]. Available: <https://arxiv.org/abs/1903.08925>
- [4] Q. Wu and R. Zhang. (Oct. 2018) Intelligent reflecting surface enhanced wireless network via joint active and passive beamforming. [Online]. Available: <https://arxiv.org/abs/1810.03961>
- [5] C. Huang, A. Zappone, G. C. Alexandropoulos, M. Debbah, and C. Yuen. (Apr. 2019) Reconfigurable intelligent surfaces for energy efficiency in wireless communication. [Online]. Available: <https://arxiv.org/abs/1810.06934>
- [6] W. Yan, X. Kuai, and X. Yuan. (May 2019) Passive beamforming and information transfer via large intelligent metasurface. [Online]. Available: <https://arxiv.org/abs/1905.01491>
- [7] J. T. Parker, P. Schniter, and V. Cevher, "Bilinear generalized approximate message passing—Part I: Derivation," *IEEE Trans. Signal Process.*, vol. 62, no. 22, pp. 5839–5853, Nov. 2014.
- [8] K. Wei, J.-F. Cai, T. F. Chan, and S. Leung, "Guarantees of Riemannian optimization for low rank matrix recovery," *SIAM J. Matrix Anal. Appl.*, vol. 37, no. 3, pp. 1198–1222, Sep. 2016.
- [9] A. Taha, M. Alrabeiah, and A. Alkhateeb. (Apr. 2019) Enabling large intelligent surfaces with compressive sensing and deep learning. [Online]. Available: <https://arxiv.org/abs/1904.10136>
- [10] Z. Gao, L. Dai, Z. Wang, and S. Chen, "Spatially common sparsity based adaptive channel estimation and feedback for FDD massive MIMO," *IEEE Trans. Signal Process.*, vol. 63, no. 23, pp. 6169–6183, Dec. 2015.
- [11] Z. Gao, L. Dai, W. Dai, B. Shim, and Z. Wang, "Structured compressive sensing-based spatio-temporal joint channel estimation for FDD massive MIMO," *IEEE Trans. Commun.*, vol. 64, no. 2, pp. 601–617, Feb. 2016.
- [12] X. Rao and V. K. Lau, "Distributed compressive CSIT estimation and feedback for FDD multi-user massive MIMO systems," *IEEE Trans. Signal Process.*, vol. 62, no. 12, pp. 3261–3271, Jun. 2014.
- [13] J. Zhang, X. Yuan, and Y.-J. A. Zhang, "Blind signal detection in massive MIMO: Exploiting the channel sparsity," *IEEE Trans. Commun.*, vol. 66, no. 2, pp. 700–712, 2018.
- [14] R. B. Green, "The general theory of antenna scattering," Ph.D. dissertation, The Ohio State University, 1963.
- [15] A. Alkhateeb, J. Mo, N. Gonzalez-Prelcic, and R. W. Heath, "MIMO precoding and combining solutions for millimeter-wave systems," *IEEE Commun. Mag.*, vol. 52, no. 12, pp. 122–131, 2014.
- [16] S. Haghighatshoar and G. Caire, "Massive MIMO channel subspace estimation from low-dimensional projections," *IEEE Trans. Signal Process.*, vol. 65, no. 2, pp. 303–318, 2017.
- [17] Q.-U.-A. Nadeem, A. Kammoun, A. Chaaban, M. Debbah, and M.-S. Alouini. (Apr. 2019) Asymptotic analysis of large intelligent surface assisted MIMO communication. [Online]. Available: <https://arxiv.org/abs/1903.08127>
- [18] P. Wang, Y. Li, X. Yuan, L. Song, and B. Vucetic, "Tens of gigabits wireless communications over E-band LoS MIMO channels with uniform linear antenna arrays," *IEEE Trans. Wireless Commun.*, vol. 13, no. 7, pp. 3791–3805, Jul. 2014.
- [19] H. Liu, X. Yuan, and Y.-J. A. Zhang. (Oct. 2018) Super-resolution blind channel-and-signal estimation for massive MIMO with arbitrary array geometry. [Online]. Available: <https://arxiv.org/abs/1810.01059>
- [20] M. Aharon, M. Elad, and A. M. Bruckstein, "K-SVD: An algorithm for designing overcomplete dictionaries for sparse representation," *IEEE Trans. Signal Process.*, vol. 54, no. 11, pp. 4311–4323, Nov. 2006.
- [21] J. Mairal, F. Bach, J. Ponce, and G. Sapiro, "Online learning for matrix factorization and sparse coding," *J. Mach. Learn. Res.*, vol. 11, pp. 19–60, Mar. 2010.
- [22] J.-F. Cai, E. J. Candès, and Z. Shen, "A singular value thresholding algorithm for matrix completion," *SIAM J. Optimiz.*, vol. 20, no. 4, pp. 1956–1982, Mar. 2010.